TECH. MEMO AERO 2146 | UNLIMITED | TECH. MEMO AERO 2146

2

ROYAL AEROSPACE ESTABLISHMENT

CFD METHODS FOR DRAG PREDICTION AND ANALYSIS CURRENTLY IN USE IN UK

by

P. R. Ashill

September 1988

Procurement Executive, Ministry of Defence
Farnborough, Hants

UNLIMITED

CONDITIONS OF RELEASE

0036829 BR-109770

.... U

.... Y

Reports quoted are not necessarily available to members of the public or to commercial organisations.

ROYAL AEROSPACE ESTABLISHMENT

Technical Memorandum Aero 2146

Received for printing 14 October 1988

CFD METHODS FOR DRAG PREDICTION AND ANALYSIS CURRENTLY IN USE IN UK

by

P. R. Ashill

SUMMARY

Computational methods developed in UK for the prediction of the drag of aircraft components at subsonic and supersonic speeds are critically reviewed. In many cases, the flow modelling isfound to be lacking in certain respects. Despite this, however, the review suggests that these methods have a useful function both in the early stages of aircraft design, when they may be used to study differences in the drag of various shapes, and later in support of wind-tunnel tests as a diagnostic tool and also to 'extrapolate' the data to 'full scale'.

LIST OF SYMBOLS

AR	wing aspect ratio
$c(\eta)$	local streamwise chord
C_D	drag coefficient based on wing planform area
$C_D(\eta)$	local drag coefficient based on local chord
C_{D_A}	drag coefficient based on surface area
$C_{D_{cowl}}$	cowl pressure drag coefficient (Fig 24)
C_{D_S}	notional drag coefficient per surface = $C_D/2$
C_{D_F}	drag coefficient based on frontal area
C_f	skin friction coefficient based on free stream dynamic pressure
C_L	lift coefficient based on wing planform area
C_M	pitching moment coefficient based on wing planform area and mean chord, nose up positive
C_p	pressure coefficient
D	drag
M	free stream Mach number
M_N	Mach number of the flow component normal to and just upstream of the shock
R	Reynolds number based on streamwise chord
S	wing planform area
T	plane normal to free-stream vector and downstream of aircraft
z	distance normal to the wing surface
α	angle of incidence
Δ	incremental part of
η	non-dimensional spanwise distance

SUFFIXES

BAL	balance measured
B	body alone
f	skin-friction component
p	normal-pressure component
TV	trailing-vortex component
V	viscous or boundary-layer component
W	wave component
WA	notional wing alone
∞	far upstream

1 INTRODUCTION

In the Technical Evaluation Report of the AGARD Conference on 'Aerodynamic Drag' held at Izmir, Turkey in April 1973, it was concluded that 'a comprehensive drag prediction method, valid for the main classes of aircraft and based entirely on theory, is not likely to be possible for a long time to come'. Fifteen years later, the wholly theoretical prediction of aircraft drag to a satisfactory standard of accuracy is still not possible. However, this period has seen considerable progress in the development of flow algorithms, notably for transonic flows, and a reduction in the cost of computations of at least two orders of magnitude[7].

These developments have encouraged the increasing use of CFD in the design of aircraft from the preliminary stages, through the development phase, to pre-production. In the early stages, approximate CFD methods (eg inviscid methods) provide the project engineer with simple tools for selecting suitable designs. Later, during the development phase, increased reliance is placed on more complex CFD methods, including, for example, viscous effects. Combined with data from carefully-conducted wind-tunnel tests, these methods enable the designer to diagnose sources of excess drag and to predict the drag of modified shapes. Used in this way, the methods need only be reliable in their predictions of small drag differences and thus it is not necessary for the flow modelling to be precise so long as the main features of the flow are represented. At this stage CFD also has an important supporting role in the wind-tunnel tests for

(i) Establishing a basis for simulating full-scale flows in the wind tunnel and, where necessary, extrapolating the tunnel data to full scale;

(ii) Calculating tunnel wall and model support interference.

Although the second application is important it is indirect and is not considered further in this paper.

Finally, before production, it is necessary to guarantee performance predictions from prototype flight-test data, and, in this phase, CFD has a possible role in the interpretation of the flight test data. Again, however, this aspect is not discussed in the paper.

This paper reviews current UK CFD methods for drag prediction. Where possible, the predictions are compared with measurement; otherwise results of calculations are included to illustrate the use of the methods in aircraft design. Because of limitations on the length of the paper the review is not exhaustive but it is hoped that the paper gives the flavour of UK activities in this field.

Following a discussion of general aspects of drag prediction in section 2, the paper reviews methods for subsonic aircraft in section 3 and for supersonic aircraft in section 4.

2 GENERAL CONSIDERATIONS

Two alternative procedures are available for obtaining drag from CFD predictions, as shown in Fig 1; the first or 'local' method involves integration of the streamwise contributions of the forces due to normal pressure and skin friction; the second is a 'field' method requiring an integration over a plane normal to the free stream and downstream of the aircraft, 'T'.

The susceptibility of the 'local' method to truncation errors is well known and results obtained by this technique should always be checked for the effect of grid spacing. The 'field' method may also be sensitive to grid density but, as yet, there is little experience on which to base a judgement of this procedure.

Investigating the drag of an aerofoil inferred from calculations by an inviscid Euler code, Yu et al[3] showed that both the 'local' and 'field' methods incorrectly gave non-zero drag for a subcritical flow. Lock[4] attributed this problem to the generation of spurious entropy near the leading edge. Thus it would appear that further development of flow algorithms is needed before the 'field' method can be used with confidence. On the other hand, with possible enhancements in mind, it may be noted that the 'field' method, unlike the 'local' method, does not depend directly on details of the aircraft geometry and may thus find an application to the prediction of the drag of complex configurations.

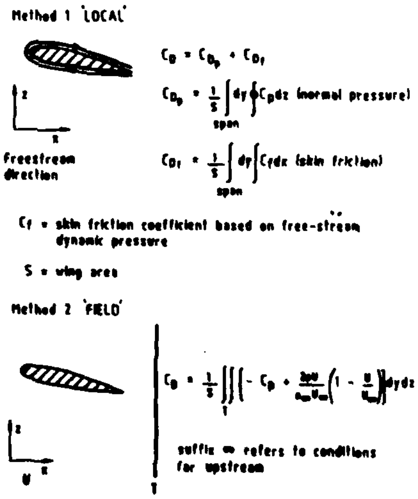

Fig.1 Two methods of determining drag

With the plane 'T' taken sufficiently far downstream, the various terms in the 'field' integral may be expanded in powers of the perturbation velocities (non-dimensionalised with respect to free-stream speed). Lock[4] showed that, to an order of approximation that is adequate for subsonic transport aircraft at cruise conditions, this expression reduces to the classical 'far field' integral which can be divided into three components as shown in Fig 2.

Lock[4] observed that the drag components of wings could be determined most conveniently and accurately by relating flow conditions at 'T' to those on or near the wing. The three drag components are treated as follows:

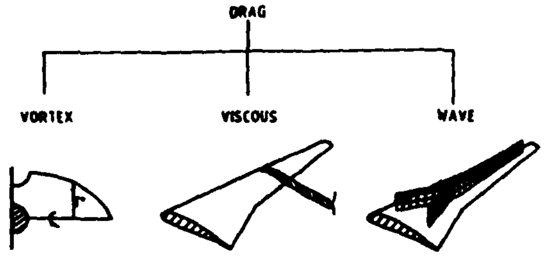

Fig.2 Far field analysis of drag of wings at subsonic speeds

(a) Wave

On the reasonable assumption that the flow downstream of all the shocks is isentropic and adiabatic, wave drag is determined by the reduction in total pressure across each element of the shock system. This statement has no meaning for potential flows but methods have been developed in UK for inferring wave drag from potential-flow solutions. A method for aerofoils at subsonic free-stream speeds due to Billing and Bocci[5], which has led to the development of the computer program known as MACHCONT, relates each element of the shock to a Rankine-Hugoniot shock of the same strength, ie having the same Mach number normal to and just upstream of the shock, M_N. Billing and Bocci also assumed that the local flow is normal to the shock. This assumption is reasonable for inviscid flows at high subsonic speeds but, in viscous flows, where the interaction beween the shock and the boundary layer causes the shock to be oblique near the aerofoil surface, the method probably overestimates wave drag.

This approach has been generalised to wing flows by Allwright[6] except that, in his method, no assumptions are made about the direction of the flow just upstream of the shock.

In cases where details of the flow field are not known or a rapid indication of wave drag is needed, a simple method due to Lock[4] is useful. In its two dimensional form, Lock's approach is similar to that of Billing and Bocci except that it uses the assumption that the shock wave lies along the normal to the aerofoil section contour. With this assumption and by retaining only the first term in the Maclaurin expansion with respect to distance from the aerofoil contour for the gradient of shock-upstream Mach number M_N normal to the aerofoil contour, Lock obtained the following expression for wave drag

$$\frac{D_W}{q} = C_{D_W}c = \frac{0.243}{k_w}\left(\frac{1 + 0.2M^2}{M}\right)^3 \frac{(M_{NO} - 1)^4(2 - M_{NO})}{M_{NO}(1 + 0.2M_{NO}^2)} \qquad (1)$$

Here M is free-stream Mach number, k_w is the local curvature of the aerofoil section at the foot of the shock, defined by the suffix O , and q is free-stream dynamic pressure.

Equation (1) implies that, for a given value of M_{NO}, section wave drag in Lock's approximation depends only on the local radius of curvature $1/k_w$. This is an appropriate length scale so long as either (a) the aerofoil curvature changes slowly upstream of the shock or (b) the height of the shock penetration into the field is small compared with $1/k_w$. Thus for wings with both a surface curvature that changes rapidly with streamwise distance and a strong shock, Lock's method may be expected to give inaccurate predictions of wave drag (see section 3.2).

Since Lock's method utilizes the assumption that the shock is normal to the aerofoil contour and is based on wing surface curvature, it does not include the effect of the viscous/inviscid interaction between the boundary layer and the shock.

Lock modified equation (1) to allow for wing sweep by using the assumption that, at each wing section, the flow is identical to that over an infinite yawed wing having the same sweep as the shock.

The determination of wave drag from solutions of the Euler equations is less straightforward than it first appears. As noted above, spurious entropy is invariably produced upstream of the shock from areas such as the wing leading edge where there are rapid changes in shape along the wing chord. Thus wave drag calculations based on the field method can be significantly in error. Attempts to infer the wave drag from the entropy rise across the shock are complicated by numerical errors in the region of the shock. Methods of dealing with this problem have been discussed by Sells[7] and Lock[4].

(b) Vortex

In order to have any reasonable prospect of calculating this component directly, it is necessary to ignore the rolling up of the trailing-vortex sheet. Considerable simplification is also possible if the downward inclination of the sheet is ignored, the resulting expression being the classical contour integral around the vortex trace in the Trefftz plane. This approach is probably adequate for high aspect-ratio wings at low to moderate lift[4] ($C_L < 0.5$) but for low aspect-ratio wings at high lift it must be of questionable accuracy.

(c) Viscous

In two-dimensional flows, viscous drag may be inferred from the solution for the viscous wake far downstream but this would not seem possible for flows over finite wings because of complications arising from wake-edge conditions[6]. Therefore, for wings, or if an accurate solution is not available for the viscous wake in two-dimensional flow, an extended version of the Squire/Young formula allowing for compressibility and wing sweep[6,8] may be used.

Unless otherwise stated, the 'far-field' method is used in drag predictions discussed later. As shown in section 3.2, this simple framework for analysis appears to be justified for subsonic transport aircraft at cruise conditions. For flows with powerful interactions between the viscous shear layers, the shock waves and the trailing vortices, a decomposition of this kind is no longer valid and the scope for diagnostic studies accordingly limited. Furthermore, overall drag would then have to be calculated using either the 'local' or 'field' methods with all the difficulties that implies.

3 METHODS FOR SUBSONIC AIRCRAFT

3.1 Aerofoils

Methods for aerofoils are viewed in UK as a first step towards the development of satisfactory flow algorithms for wings and, as such, have been used to test ideas on various aspects of flow modelling. However, aerofoil methods have progressed to the point of being powerful design tools in their own right and are currently used for tasks such as:

(i) selection of wing sections;

(ii) design of flaps and slats; and

(iii) extrapolation of tunnel data to 'full scale'.

The majority of the methods currently in use in UK (Fig 3) are of the viscous/inviscid interaction type in which calculation of the two parts of the flow is performed interactively and iteratively to numerical convergence. A number of numerical schemes are used, namely Direct (which is only suitable for attached flow), Semi-Inverse (SI) (which may be used for separated flows) and Quasi-Simultaneous (QS) (which is equally effective for both separated and attached flows). Full details of these schemes are given in the review by Lock and Williams[9].

In the remainder of section 3.1, the methods summarised in Fig 3 are reviewed, methods for low speed (and high lift) being considered in section 3.1.1 and techniques for high subsonic speeds in section 3.1.2.

a) Low-speed methods

CODE	ORIGINATORS	INVISCID	ALGORITHMS —COUPLING—	VISCOUS
SIVP	Williams[10]	Source panel	—(SI)—	LE method[11]
HILDA	Newling[16] Butter & Williams[14]	ditto	—(direct)—	LE method[11] plus Irwin's[17] or Cross's[18] method for merging wakes
FELMA	King & Williams[19]	Finite element soltn. of full potential eqn. 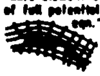	—(QS or SI)—	LE method

b) High-speed methods

CODE	ORIGINATORS	INVISCID	COUPLING	VISCOUS
VISTRAN	Firmin & Jones[22]	Finite difference soltn. of transonic small perturbation eqn. 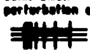	—(direct)—	LE method
VGK	Collyer & Lock[21]	Quasi-conservative finite difference soltn. of full potential eqn. 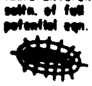	—(direct)—	LE method
BVGK	Ashill, Wood & Weeks[23]	ditto	—(SI)—	Modified LE method
BAe Euler code	Doe, Pagano & Brown[26]	Finite volume soltn. of Euler equations 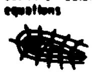	—(SI)—	ditto

LE = Lag Entrainment

Fig.3 U.K. CFD methods for aerofoil drag prediction

3.1.1 Low speed

UK methods for calculating drag and maximum lift of aerofoils at low free-stream speeds may be summarised as follows:

(1) SIVP (Semi-Inverse Viscous Program)

This method[10] is restricted to single aerofoils, and, as its name suggests, utilises an SI scheme, with a surface-singularity technique for the inviscid flow and integral methods for the shear layers. The turbulent boundary-layers are calculated by the lag-entrainment method[11] while the laminar layers are computed using a compressible version of Thwaites' method[12].

Further allowance is made in the turbulent boundary-layer calculation for the effect on skin friction of low Reynolds-number (ie a local value of momentum-thickness Reynolds number, R_θ, less than about 1000). However, R_θ is not allowed to fall below 320 just downstream of transition, since this a natural limit for a fully-developed turbulent boundary-layer. In addition, the secondary influence of flow curvature on turbulence structure is included in the 'lag' equation.

Finally, the standard shape-parameter relationship[11] is replaced by one that is more suitable for separated flows[9]. No allowance is made for the 'higher-order' effects in the streamwise momentum equation due to normal pressure gradients and Reynolds normal stresses. The latter 'higher-order' effect, which is the more important of the two, is not included because correlations of it[13] are of doubtful validity for flows with extensive regions of separation.

While the method gives close predictions of maximum lift, as illustrated for two different aerofoils in Fig 4, it predicts much lower drag than that measured on the aerofoil GA(W)-2 (Fig 5). This discrepancy might be explained by results of calculations which suggest that the transition trips used in this experiment were not adequate over the entire range of incidences tested[9]. The neglect of the Reynolds normal-stress term mentioned above may also be significant.

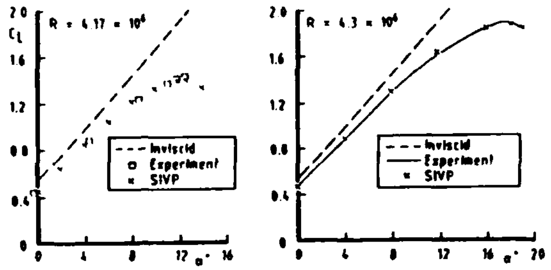

(a) NACA 4412 (b) GA(W)-2

Fig 4 Variation of lift coefficient, C_L, with angle of incidence, α, for two aerofoils

The viscous 'package' in this program has been written so that it can readily be coupled with other inviscid methods, and it has also been used in the FELMA and British Aerospace (BAe) Euler codes described later.

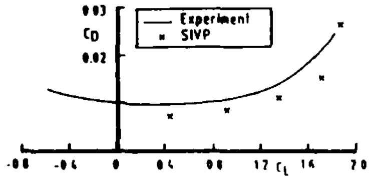

Fig 5 Variation of C_D with C_L for GA(W)-2 aerofoil, $R = 4.3 \times 10^6$

(ii) HILDA (High Lift Design and Analysis)

Developed to calculate flows over multi-element aerofoils, this method[14] uses the Direct coupling scheme of the earlier MAVIS[15] (Multiple Aerofoil Viscous Iterative System) program but has an improved surface-singularity method for the (incompressible) inviscid flow[16]. As in SIVP, the turbulent boundary-layers and isolated wakes are calculated by the lag-entrainment method. No allowance is made for 'higher-order' effects in the streamwise momentum equation but a correction for the influence of low Reynolds number on turbulent skin-friction is included.

Merging of the wakes from upstream elements with boundary layers is calculated by the integral method of Irwin[17] and more recently by a method due to Cross[18].

Since the Direct scheme is used, the method fails where separation occurs and thus bubble separations occurring in re-entrant or 'cove' regions are empirically modelled.

Predictions of lift and drag for a three-element aerofoil are shown in Fig 6. The viscous-induced loss in lift is well predicted for angles of incidence, α, up to 20° but, at higher angles, the flow separates on the main aerofoil and consequently the method fails. In Ref 9 it is argued that the good agreement between calculations and measurement at $\alpha = 20°$ is to some extent fortuitous, the lift on the main aerofoil being overestimated while the lift on the other two elements is underestimated.

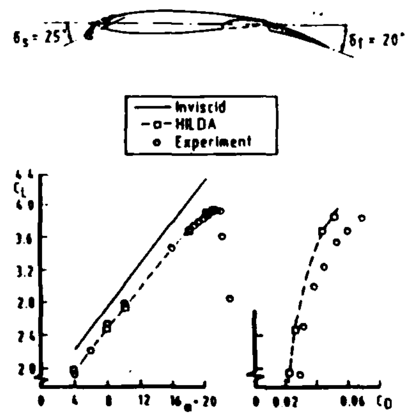

Fig 6 Variation of lift with angle of incidence and drag for a multi-element aerofoil

The estimates of drag are far less satisfactory especially as the stall is approached. As well as the omission of 'higher order' effects referred to above, possible reasons include the lack of compressibility effects in the calculation of the inviscid flow and the inadequacy of the modelling of the aerofoil wake in the region of high flow-curvature above the flap.

(iii) FELMA (Finite Element Multiple Aerofoil)

As implied above, compressibility can exert a significant influence on low speed flows over multiple-element aerofoils at high lift particularly where the flow accelerates to high speeds locally, eg at the leading-edge slat. FELMA[19] represents compressibility in the inviscid flow by solving the exact potential equation numerically by a finite-element technique. As noted previously, the viscous shear layers are calculated by the method used in SIVP but, in contrast to HILDA or MAVIS, FELMA does not represent the merging between wakes and boundary layers. The option is provided to use either SI or QS couplings, allowing flows with separation to be calculated. Of the two schemes, QS is the more efficient, being faster than SI and not requiring a switch from Direct coupling for the attached portion of the flow to SI coupling in regions of separation.

Comparisons of predictions by FELMA and measurements of lift and drag are shown in Fig 7 for the NLR 7301 aerofoil/flap configurations 1 and 2, having, respectively, flap gaps of 2.6% and 1.3% basic aerofoil chord. The calculation of maximum lift is in reasonable accord with measurement for the larger of the two flap gaps but for the smaller gap the maximum lift is overestimated, possibly because an observed interaction between the aerofoil wake and the flap boundary layer is not represented in FELMA.

While some encouragement can be drawn from the drag predictions in Fig 7, it should be noted that the NLR configurations are somewhat idealised in that they do not represent a 'cove' on the main aerofoil. It remains to be seen if FELMA offers improved accuracy over that of HILDA for more practical configurations where the merging of wakes from upstream elements and boundary layers may be an important feature of the flow.

Overall, the present situation in UK as regards the prediction of drag of high-lift aerofoils is not altogether satisfactory. There are reasons to believe that this arises because of defects in the modelling of the wake of the main aerofoil in the region of high flow-curvature above the flap. In this region both streamwise and crosswise pressure gradients are large and hence the flow there is highly elliptic in character. Thus, in order to achieve the required accuracy, it may be necessary to use one of the new generation of methods for solving the Reynolds-averaged, Naviers-Stokes equation[20]. However, these methods will only be able to provide the necessary accuracy if turbulence models are found which are suitable for highly-curved wakes[19].

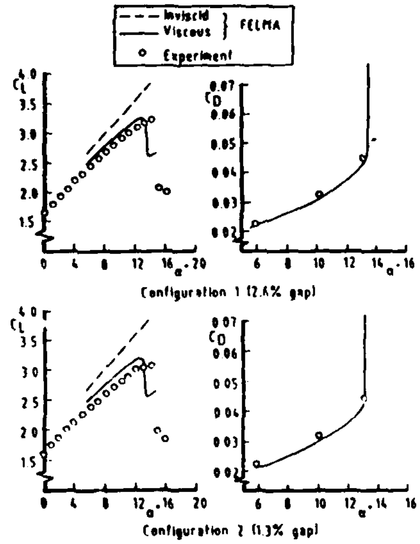

Fig 7 Lift and drag versus incidence. NLR two element (aerofoil/flap) configurations. $R = 2.5 \times 10^6$, $M = 0.185$

3.1.2 High speed

Because of the importance of being able to estimate accurately section drag for transport-type wings, emphasis has been placed in UK on the development and validation of transonic-flow codes (Fig 3). Methods currently favoured include those based on the assumption that the inviscid flow is potential and others in which the Euler equations are used to simulate the 'outer' flow.

(i) Methods using potential-flow approximation

The code VGK[21] has been the mainstay of wing section design and analysis in UK for over ten years, having superseded the transonic small-perturbation code VISTRAN[22]. VGK couples, in the Direct way, a numerical solution of the full-potential equation with integral methods for the shear layers, the laminar and turbulent layers being calculated, respectively, by Thwaites method[17], extended to allow for compressibility, and the lag-entrainment method[11].

In general, VGK gives satisfactory predictions of drag for attached flows but, where flow separation is approached, the method underestimates drag by a significant margin as shown later. The cause can be traced, in part, to the neglect of 'higher order' effects in the streamwise momentum equation and in the matching between the viscous and inviscid flows. A revised version of the program, known as BVGK, has therefore been developed[13] including these effects together with corrections to the lag-entrainment method similar to those in SIVP described previously. (A slightly different shape-parameter relationship from that of SIVP is used which is considered to be suitable for flows with trailing-edge separation).

Drag is calculated in BVGK by both the 'local' and 'far-field' methods. However, for reasons given in section 2, the 'far-field' method is generally preferred, and predictions of drag by BVGK and VGK shown later have been obtained in this way, using MACHCONT as the subroutine for wave drag.

Examples of predictions by VGK and BVGK of overall forces and pitching moment are shown in Fig 8 for a series of 14% thick aerofoils with relatively-large rear loading. This figure is taken from Ref 23 where details are given of the aerofoils and the wind tunnel measurements used in the assessment of CFD methods. Here it suffices to note that, at the lower of the two chord Reynolds numbers, $R = 6 \times 10^6$, flow separation is calculated by BVGK to occur on the upper surface of three of the aerofoils, RAE 5225, 5230 and 5234, the chordwise positions of the separation point being at 99%, 95% and 98%, respectively, for $C_L = 0.4$. Hence these flows present a challenge to CFD methods for predicting drag.

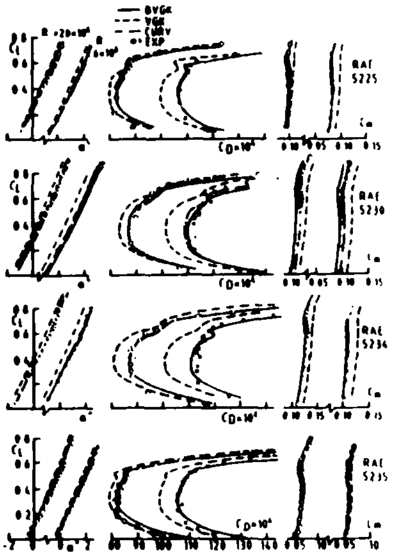

Fig 8 Lift, drag and pitching moment curves M ≈ 0.735 R = 6 × 10⁶ & 20 × 10⁶ (17.7 × 10⁶ RAE 5230)

Fig 8 reveals that the predictions of drag by BVGK are in good agreement with measurement for flows with weak shocks at both Reynolds numbers. Therefore, by implication, BVGK predicts accurately the differences in drag between sections at a given Reynolds numbers and between Reynolds numbers for a given section. The improvement in agreement with measurement compared with the predictions by VGK is especially evident at $R = 6 \times 10^6$, where, as noted before, separation is calculated to occur on the upper surface of three of the aerofoils. However, the drag estimates by BVGK are less satisfactory where there is significant wave drag ($\Delta C_{DW} > 0.001$). Two possible explanations are given in Ref 23, one related to the fact that MACHCONT assumes that the local flow is normal to the shock wave and the other to the tendency for BVGK to underestimate the rear loading for flows with significant rear separation (notably RAE 5230). A study of possible causes for the latter effect suggests that the correction to turbulence structure for flow curvature is of doubtful validity for separated flows and is probably best ignored in such cases. The result of neglecting this correction is shown in Fig 8 for RAE 5230, the modified calculation being referred to as -CURV. The improved predictions of rear loading with -CURV lead to estimates of pitching moment and drag at the 'drag rise' condition in better agreement with measurement.

A version of VGK is available with allowance for wing sweep. Known as SWVGK, this method[24] represents the influence of cross flow on the shear layers but does not include effects allowed for in BVGK, which are known to become important for unswept aerofoils as separation is approached.

The accuracy of the predictions by this method and also by VGK and BVGK of drag differences between sections and between Reynolds numbers have been studied by comparison with data from a panel wing swept at 25°. In this assessment, the effect of sweep on drag in VGK and BVGK is allowed in a simple way as discussed in Ref 23 which also describes the aerofoil sections and the wind-tunnel tests. Here it may be noted that (a) section drag was determined by the wake-rake technique and (b) the wing was cylindrical, of symmetrical section and was tested at zero lift.

Comparisons are shown in Fig 9 between predictions and measurement for the difference in the notional drag-coefficient per surface $C_{DS} = C_D/2$ between the two sections RAE 5237 and 5238 over a range of Mach numbers. These sections are related through calculated boundary-layer characteristics close to the trailing edge to the unswept aerofoil sections RAE 5225 and 5230 (see Fig 8). Of the three methods, the best agreement with measurement is obtained with BVGK, suggesting that the effects shown to be important for unswept aerofoils as separation is approached have a similar significance for wings of moderate sweep.

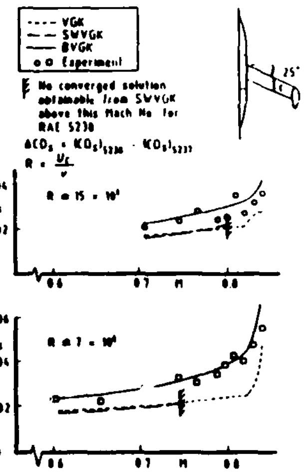

Fig 9 Notional drag per surface of RAE 5238 relative to that of RAE 5237, swept panel model

The effect on the variation with Mach number of the drag coefficient C_{DS} of changing chord Reynolds number from 6.5×10^6 to 14×10^6 is shown in Fig 10. Again, the closest estimates of this change are obtained with BVGK and this figure taken together with Fig 8 shows that BVGK has a potentially-useful role in the extrapolation of wind-tunnel data to 'full scale', at least for wings of moderate sweep and high aspect ratio.

(ii) Methods based on the Euler equations

A code for the numerical solution of the Euler equations based on the finite-volume method of Jameson et al[25] has been written at BAe Filton[26]. To permit detailed comparison with experiment, allowance has been made for viscous effects via the method due to Williams[10] ie, using an SI coupling and including certain 'higher-order' effects. Drag is computed using the 'far-field' method, the wave drag being inferred from the loss in total pressure across the shock in the way suggested by Sells[7].

Only limited comparisons with measurement have been published but these indicate that the method gives accurate predictions of drag for the sections RAE 5225 and 5230 at high Reynolds number (Fig 11).

Recently, Hall[27] has developed a multi-grid scheme for solving the Euler equations which when combined with techniques similar to those mentioned above for solving the shear-flow equations, promises a method for calculating viscous transonic flows over aerofoils that can represent shock waves accurately while being no more costly to run that BVGK.

Johnston[28] has described a method for solving the Reynolds-averaged, Navier-Stokes equations for the transonic flow around aerofoils which is based on the work of Weatherill et al[30] for multiple aerofoils. In this method, Reynolds stresses are modelled using the eddy-viscosity hypothesis combined with an algebraic turbulence-model. Thus the method is probably not reliable for predicting drag for cases with regions of separation near the trailing edge such as those considered previously.

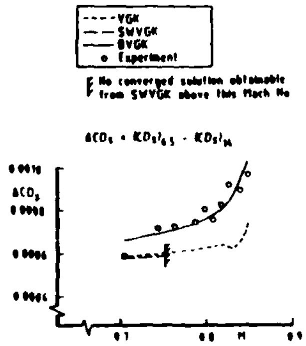

Fig 10 Differences between notional drag per surface at two unit Reynolds numbers. $R = 6.5 \times 10^6$ and $R = 14 \times 10^6$, RAE 5230

3.2 Wings

UK methods for wings are either inviscid or are of the viscous inviscid interaction type. The viscous versions of these methods are not as advanced as those for aerofoils in the treatment of effects which are significant for flows that are close to separation and consequently cannot yet predict the drag of modern wings with the accuracy demonstrated in Figs 8 to 11. Generally, the viscous versions use Direct coupling, although SI coupling is employed in an approximate way in one method (see later). Despite lacking the accuracy of the aerofoil methods, wing techniques, used with caution and experience, are invaluable aids to design, providing the facility to identify and minimise three-dimensional sources of excess drag.

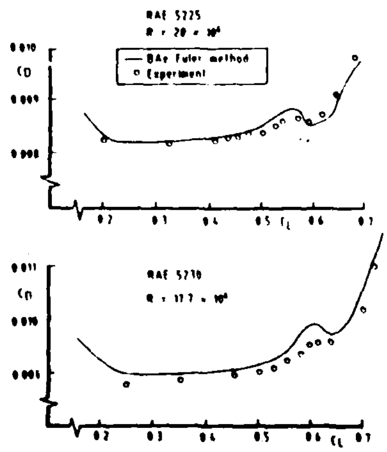

Fig 11 Variation of drag coefficient with lift coefficient. M = 0.735

Fig 12 tabulates the methods. Of the panel methods,[29,30,31,32] that due to Petrie[32] (SPARV) appears to be the most used and is the subject of continuing development. Allowance is included in this method for the effect of wing boundary layers[33]. The inviscid transonic, small-perturbation method of Albone et al[34], with viscous effects incorporated by Firmin[35], is now largely superseded by the more accurate full-potential and Euler methods. The full-potential method of Forsey and Carr[36] (FP) has been used for several years and is generally regarded as a good example of a method of this type. A version of the method, due to Arthur,[37] is available with allowance for viscous effects (VFP). Finally, BAe Filton have programmed a three-dimensional version of the Euler method referred to in section 3.1.2; in this method[26], the shear layers are calculated on the assumption of planar flow at each streamwise section with the solution coupled to the inviscid-flow solver by an SI scheme.

Few results of comparisons of drag predictions by these methods with wind-tunnel experiment are available for publication, and consequently the remainder of the section is concerned with methods of analysing the drag of wings from information provided by the codes based on the classical 'far-field' approach described in section 2. Results of analysis are presented to illustrate the power of this approach in identifying sources of excess drag.

An analysis of drag is shown for a wing/body suitable for a transport aircraft comprising a wing of aspect ratio 8, with a leading-edge sweep of 28° and a trailing edge sweep outboard of the trailing-edge crank of 14° (Fig 13). In addition, a study of wave drag is presented for a wing representative of that of a subsonic combat-aircraft having leading and trailing edge sweeps 39° and 15° and an aspect ratio 3.3.

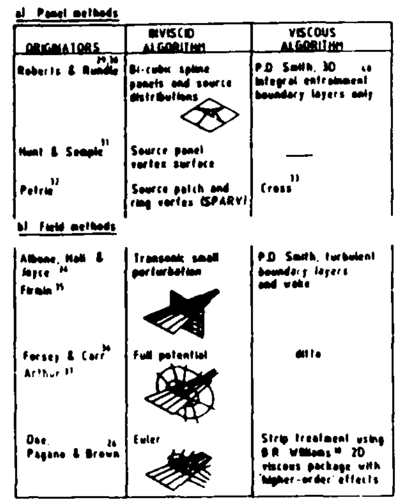

Fig 12 UK CFD methods for wings

(i) Transport aircraft configuration

Comprehensive CFD calculations are not available for this configuration and so the analysis is performed using wing surface pressures measured on a complete model[8]. Limited calculations of wing pressures for this configuration by both the BAe[26] and VFP[37] codes have been found to be in reasonable agreement with measurement (made in the latter case on a related half model).

The form of analysis is illustrated in Fig 14. The body-drag coefficient C_{DB} is determined from tests on the body alone, thereby avoiding the difficulty of determining sting interference. Note that, in choosing the ordinate for this figure, use is made of the fact that the vortex drag is close to the minimum value for a planar wing by subtracting from the drag coefficient $C_{L_{BAL}}^2/\pi A$, where A is wing aspect ratio and suffix BAL refers to force-balance measurement. The small excess vortex-drag coefficient.

$$\Delta C_{DTV} = C_{DTV} - C_L^2/\pi A$$

is determined from the measured span loadings using the classical Treffz-plane method referred to in section 2. Two alternative vortex-trace models have been considered, one allowing for the body in a simple way and the other representing the trace as a planar slit of the same span as the wing. The latter model was chosen for the analysis on the basis that it yields values of overall lift in closer agreement with the balance-measured values than those of the other model. However, the excess vortex drags given by the two models do not differ by much ($\Delta C_D < 0.0002$) suggesting that, where overall lift is known accurately from some other source (in this case the force balance), the drag analysis is not sensitive to the shape of the vortex trace.

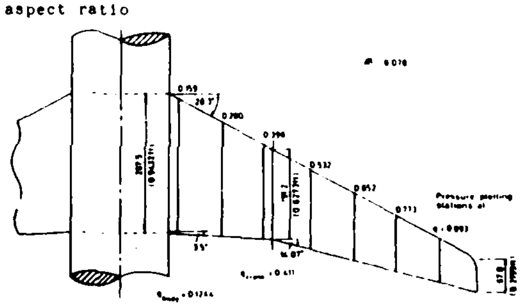
Fig 13 Planform of wing W4 showing pressure-plotting stations

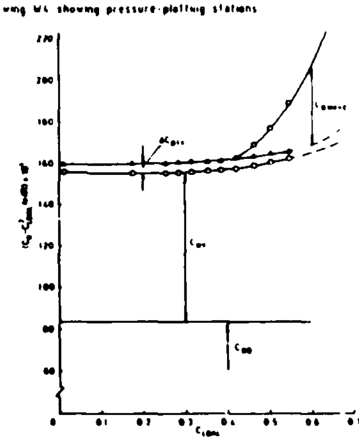
Fig 14 Analysis of drag M = 0.78

Calculated values of ΔC_{DTV} are shown in Fig 15 plotted against lift coefficient for various Mach numbers. Except where there is a rapid increase in vortex drag with lift, the excess vortex drag varies slowly with both lift and Mach number, the sudden increase being attributed to the loss in lift on part of the outer wing following flow breakdown.

Except in special cases, the integrand of the vortex-drag integral or 'local' vortex drag cannot be related to sectional drag; however there is a direct relationship between 'local' vortex drag and span loading, and, in the present case, the cause of the non-zero excess vortex-drag is that the outer wing is relatively lightly loaded compared with the ideal elliptic loading.

As is well known, the vortex drag of wings with non-planar vortex traces (eg wing/winglet configurations) can be below the minimum for planar wings of the same span, and a technique for calculating the minimum vortex drag of non-planar configuration has been programmed by Isaacs[18].

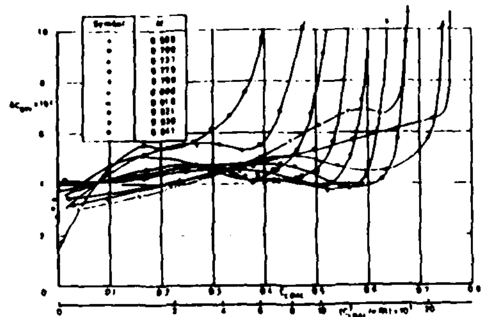

Fig 15 Excess vortex drag

As noted in section 2, viscous drag is inferred from boundary-layer quantities at the trailing edge using an extended version of the Squire-Young formula[8]. The turbulent boundary-layers are calculated using the measured pressure distributions and an 'infinite tapered wing' version[19] of the lag-entrainment method. Comparisons with the potentially, more-accurate, three-dimensional of Smith[20] suggests that the 'infinite tapered-wing' method simulates adequately three-dimensional effects in the present case except close to the tip and the root.

Typical spanwise distributions of local viscous-drag coefficient $C_{DV}(\eta)$ are illustrated in Fig 16, for M = 0.78. The relatively-large increase in local viscous-drag coefficient on the outer wing as lift coefficient increases from 0.42 to 0.55 is consistent with the growth in shock strength with lift and the consequent thickening of the boundary layer downstream of the shock on this part of the wing. The magnitudes of the local contributions to overall viscous drag are indicated in Fig 16 by $C_{DV}(\eta)c(\eta)/\bar{c}$, where c is local streamwise chord and $\bar{c}$ is geometric mean chord.

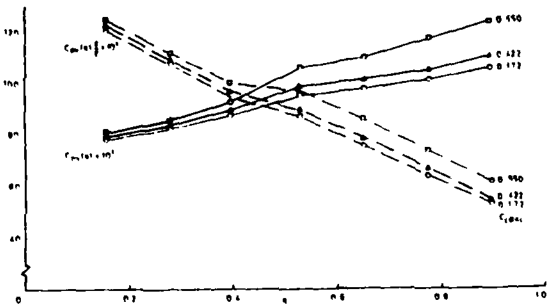

Fig 16 Spanwise variation of viscous drag M = 0.78

In the absence of flowfield information, wave drag has been calculated by Lock's method[21]. It will be recalled from section 2, that, in this method, the variation of shock strength with distance normal to the wing surface is determined by wing streamwise curvature and static pressure at a point just upstream of the shock. This is equivalent to ignoring the effect on flow curvature of the boundary layer and assuming that the strength of the shock in the field is unaffected by the variation of surface curvature along the chord upstream of the shock. These aspects are considered again in the second example in which there is a rapid variation of streamwise curvature ahead of the shock on part of the wing. However, in the present case, the curvature of each wing section is close to a minimum in the region of the shock.

Spanwise variations of the local wave-drag coefficient $C_{DW}(\eta)$ calculated by Lock's method are shown in Fig 17 together with the local contribution to wave drag $C_{DW}(\eta)c(\eta)/\bar{c}$ for M = 0.78. The contribution to wave drag of the part of the wing inboard of the trailing-edge crank is seen to be relatively small, with most of the wave drag originating from a region just outboard of the crank.

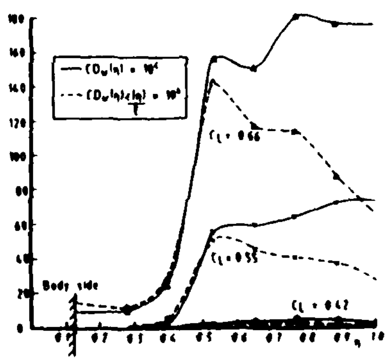

Fig 17 Spanwise distribution of normalised local wave drag coefficient, M = 0.78

Both local viscous and wave drags have been integrated across the wing span and have then been combined with vortex drag and body drag as shown in Fig 18 to give overall drag. Comparisons between 'calculated' and measured overall drags are shown in Fig 18 and indicate that, for subcritical flows or in the region of minimum drag, the 'calculated' drag coefficient is lower than the measured value by an amount which varies between 0.0004 at M = 0.6 and 0.0008 at M = 0.8. Although in less good agreement with measurement than BVGK is found to be for a series of aerofoils (Fig 8), these estimates are encouragingly close to measurement and show that the 'far-field' method has a useful role to play in the analysis of drag of wing/body configurations suitable for transport aircraft. A study of the sources of the discrepancies[8] suggests that the errors can be largely explained by flow features not represented completely in the analysis including:

(a) wing/body, boundary-layer interference;

(b) flow curvature and Reynolds normal stresses in the turbulent shear layers; and

(c) transition-trip drag.

Fig 18 reveals that the differences between 'calculated' and measured drags decrease as wave drag increases for Mach numbers in the range 0.7 to 0.81. The most likely explanation for this is that Lock's method overestimates wave drag, since it is unlikely that the estimates of the other two drag components become more accurate as shock strength increases. On the evidence of studies of inviscid, two dimensional flows it is stated in Ref 40 that estimates by Lock's method are probably within -10 to 30% of the correct value except at low values of C_{DW} (< 0.0015) when it could be up to 0.0005 too high. No direct evidence is available on the effects of the boundary layer or three-dimensionalities in the flow. However, some comparisons have been made between predictions by Lock's method and those of Allwright's field method[6], in each case based on calculations by the FP method of Forsey and Carr[36] for the present configuration. These comparisons reveal that three-dimensional effects are significant only in the near vicinity of the tip (ie within about one or two chords) and thus, overall, their influence on wave drag may be ignored.

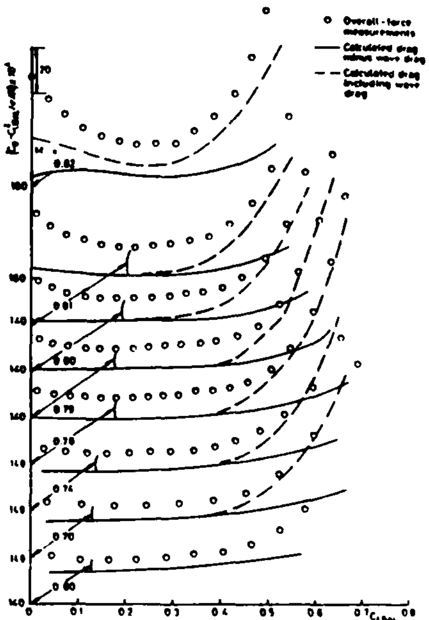

Fig 18 Comparison between 'calculated' and measured drags

(ii) Combat aircraft wing

The second configuration is an example of a wing design for which Lock's method - at least in its present form - is less reliable. The wing has been tested as a half model with the aim of providing fluid-dynamic data for the validation of CFD methods. Comparisons of predictions by VFP and measurements of wing pressure distributions are discussed in Ref 9. As part of this study, M. C. P. Firmin (RAE) has performed some calculations of wave drag using both Lock's and Allwright's techniques. Results for local wave-drag are shown in Fig 19. Outboard of the shock bifurcation at η = 0.45, Lock's method is seen to give much larger values of local wave-drag than those of Allwright while, further inboard, Lock's predictions for the rear shock are slightly lower on average than Allwright's values. An explanation for the former discrepancy is given in Fig 20 which shows the variation with distance from and normal to the wing surface of shock-upstream Mach number.

At η = 0.604, ie outboard of the bifurcation, Lock's method predicts that the shock penetrates much further into the field than is indicated by the more-accurate field method of Allwright. The reason for this is that the curvature of the wing upper-surface increases markedly with distance upstream of the shock on this part of the wing. Thus the flow curvature at the shock in the field is affected (via the outgoing Mach characteristics from the wing surface) and consequently the rate at which M_N changes with distance normal to the wing is modified.

Fig 20 also shows that, close to the wing surface, where the flow is strongly influenced by conditions at the foot of the shock, there is a marked difference in the two predictions of the variation of M_N with distance from the wing. This discrepancy arises from the neglect of the effect of the boundary layer on (a) the local flow curvature and (b) the inclination of the shock relative to the wing surface.

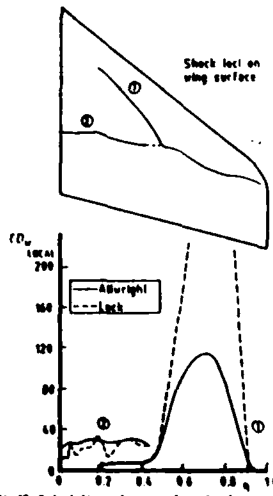

Fig 19 Calculation of wave drag by two methods. M = 0.88, C_L = 0.392

Despite these deficiencies, Lock's method is useful in providing a rapid indication of sources of excess drag both in the early stages of the wing design and later on as a diagnostic tool following wind-tunnel tests.

3.3 Bodies

Perhaps the first UK attempt to use CFD for the prediction of body drag was by Myring[42] who employed a viscous/inviscid interaction technique to calculate the subcritical flow over axisymmetric bodies at zero incidence. He represented the inviscid flow over the displacement surface of the body and the shear layer by a source-ring method and calculated the viscous shear-layers by integral methods, coupling the two solutions by a Direct procedure.

Using his method, Myring was able to design a 'low-drag' body, as illustrated in Fig 21, where it is distinguished from a conventional body of the same thickness ratio in having no pronounced suction peaks. Also shown in this figure is the variation with thickness ratio of drag-coefficient based on surface area, C_{DA}, for both types of body, clearly illustrating the superiority of the 'low drag' design, albeit at the expense of a lower body-volume. On the other hand, the 'low-drag' body has somewhat higher suctions or local velocities than those of the conventional shape in the region where the wings of an aircraft might be mounted, showing the danger of optimising aircraft components in isolation.

A number of methods have been developed in UK for calculating transonic flows over bodies, including the full-potential method of Baker and Ogle[43] for axisymmetric bodies and two methods of solving the Euler equations for the flow over forebodies.

Baker's method has been used[44] to calculate the variation of drag with Mach number of spherically-blunted forebodies at zero incidence for Mach numbers up to the limit of validity of the method, ie approximately unity. An example[44] of the reasonable agreement between predictions by this method of pressure distributions and drag is provided by Fig 22. Drag is inferred from the calculation by the 'local' method and a small tare correction to allow for discretisation errors in the method and skin-friction drag is applied to the theory to align prediction and measurement at $M = 0.7$.

Corresponding calculations of drag by the first of the Euler methods[45] are also shown in Fig 22. Based on the BAe algorithm for solving the Euler equations, this technique is applicable to axisymmetric forebodies[26]. Again the predicted variation of drag (by the 'local' method) with Mach number in the subsonic range is in fair agreement with measurement. This method has been generalised by BAe[26] to include forebodies of general shape at incidence, and a further generalisation has been performed by Aircraft Research Association, (ARA) Bedford[46] who have applied their multiblock technique to enable sideslip to be considered. Pressure distributions on the upper and lower sides of the body calculated by the latter method are compared with measurement for the forebody of the BAe Hawk at incidence and sideslip angle β in Fig 23. No comparisons of drag are available but the agreement between calculated and measured pressure distributions is reasonably good, suggesting that the method may be used to calculate the variation of drag with Mach number for such shapes.

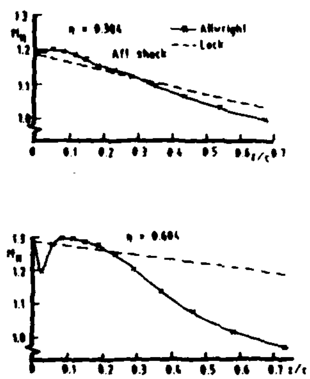

Fig 20 Calculation of Mach number normal to shock at two stations on wing

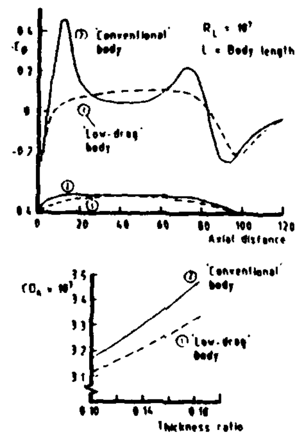

Fig 21 Pressure distributions and drag versus thickness ratio for axisymmetric bodies calculated by Myrings method

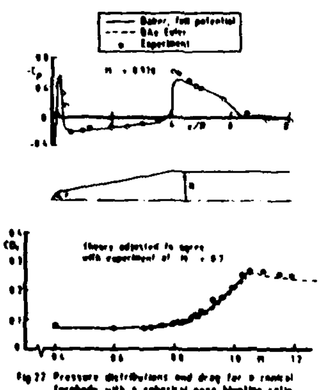

Fig 22 Pressure distributions and drag for a conical forebody with a spherical nose blunting ratio r/R = 0.3

Techniques such as the last one have yet to be combined interactively with boundary-layer calculation methods to predict the drag of general bodies. Of particular interest in this connection are fuselages with upswept afterbodies.

3.4 Cowls and nozzles

The accurate calculation of turbofan cowl drag is an important consideration in the design and the performance prediction of modern transport-aircraft. To be fully representative, the calculation method should simulate the interaction between the engine, the pylon and the wing. This cannot be done, at present, although progress is being made in the modelling of complex configurations (section 3.5) but, as a preliminary to obtaining solution to the complete problem, two methods have been programmed for isolated cowls. These methods have a similar function to that of aerofoil methods in providing a simple basis for checking flow algorithms. The first method, due to Peace[47], uses a direct coupling of a full-potential solution of the inviscid flow with the lag-entrainment method for the turbulent boundary layers. The second procedure replaces Peace's potential-flow scheme by the BAe method for solving the Euler equations[25].

Goldsmith[48] has made comparisons between predictions by these methods and measurements of cowl pressure drag for a number of NACA-1 cowls aligned with the free stream. Comparisons for the cowl geometry sketched in Fig 24 are shown in Fig 25 where cowl pressure-drag coefficient is plotted against the relative-flow ratio A_∞/A_c as defined in Fig 24. Peace's method is limited to Mach numbers below about of unity, and in this Mach-number range it gives good agreement with measurement for relative-flow ratios above those for which cowl-lip separation occurs. For low relative-flow ratios, the agreement is less satisfactory, as might be expected for a method using a first-order treatment of the shear layers.

The Euler method has only been used for calculations at supersonic speeds and so a discussion of these comparisons is deferred until section 4 where methods for supersonic flows are discussed.

A number of methods have been produced in UK to calculate the drag of afterbodies with propulsive jets. Hodges[49] has considered the case of an axisymmetric afterbody with a single jet and simulates the external flow by a panel method, the jet by the method of characteristics and the boundary layer with the lag-entrainment method. Thus the method is restricted to uniformly-subsonic external flows and jet flows which are entirely supersonic. The solutions to the various parts of the flowfield are patched and empirical relationships are used to define the separation and reattachment points and also the entrainment in the mixing region. Comparisons of prediction by two methods[50], including Hodges' method, and measurements of afterbody pressure drag for a series of nozzles, at various jet-pressure ratios and for M = 0.6 and 0.8, reveal that Hodges' method is in reasonable agreement with measurement for subcritical external flows.

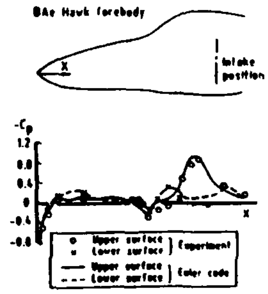

Fig 23 Upper and lower body pressure distributions, BAe Hawk forebody, M = 0.8, α = 3.72°, β = 9.14°

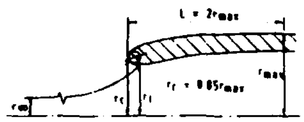

A_∞ = Streamtube cross-sectional area far upstream $= \pi r_\infty^2$

A_c = Cowl highlight or capture area. $= \pi r_c^2$ (= 0.73 A_{max})

$A_{max} = \pi r_{max}^2$

$$C_{D_{cowl}} = \frac{2\pi}{A_{max}} \int_{r_c}^{r_{max}} C_p r\,dr$$

Fig 24 Cowl geometry and definitions

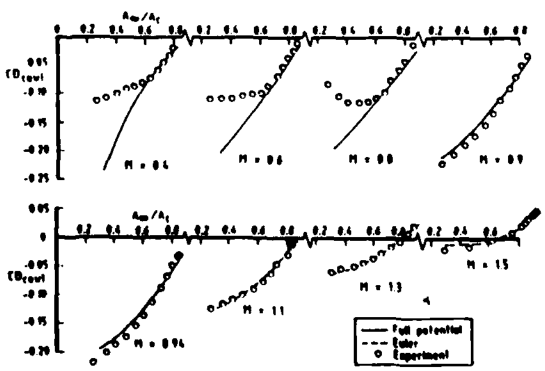

Fig 25 Cowl pressure drag as a function of capture ratio and free-stream Mach number

Peace[51] has developed a method based on solutions of the Euler equations in both the external flow and the jet which is not restricted to subcritical flows outside the jet. As in Hodges' procedure, the boundary layer is calculated by the lag-entrainment method[11] but replaces the Direct coupling and empirical separation prediction of Hodges' technique by an SI coupling. On the other hand, the entrainment in the jet mixing region is determined by a simple empirical correlation.

Fig 26 shows plots of afterbody pressure-drag coefficient against free-stream Mach number for an afterbody nozzle configuration tested by Reubush and Runckel[57]. The predictions by the method of Peace are seen to be in good agreement with measurement except close to M = 1.

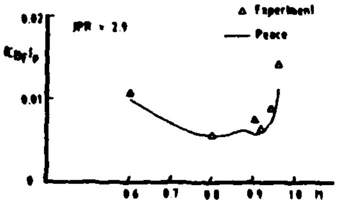

Fig.26 Pressure drag coefficient against M on Reubush and Runckel afterbody nozzle configuration 3

3.5 Complex configurations

The requirement to be able to calculate transonic flows around complex configurations, such as those shown in Fig 27, has led to the development at ARA, Bedford[53,54] and at BAe of multiblock grid generation schemes. Combined with the BAe technique for solving the Euler equations, these methods have been used for the calculation of the flow over a wide variety of configurations, an example being given in section 4. However, assessment of drag predictions by the method is still at an early stage, and, as noted in section 2, the production of spurious entropy by the current generation of Euler solvers makes the accurate determination of drag difficult; nevertheless it is envisaged that possible applications of the method in the future include:

(i) determination of the installed drag of pylon/cowl or weapon arrangements;

(ii) calculation of trimmed drag of closely-coupled configurations; and

(iii) calculation of drag of wing/winglet combinations.

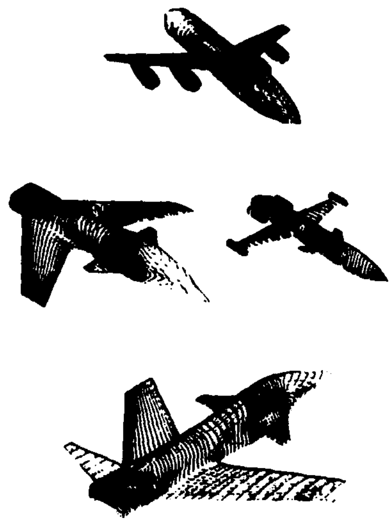

Fig 27 Surface grids for a variety of aircraft configurations

4 METHODS FOR SUPERSONIC AIRCRAFT

The airframe components of supersonic aircraft are generally integrated closely and hence the aerodynamic interference between them can be considerable. Consequently this section is different from the preceding section in that no distinction is made between components and the methods are considered under separate headings in chronological order of development.

4.1 Generalised near field wave drag program

The discovery that methods based on 'area transfer' rules do not give reliable predictions of zero-lift wave drag led BAe (Warton) to produce a code based on a simplified panel method for linearised supersonic-flow known as the Generalised Near Field Wave Drag (GNFWD) program[55]. Sufficient confidence has been established in the accuracy of the method for a range of military combat-aircraft configurations for it to be used in a routine way on project design. An application is illustrated in Fig 28; the design exercise involved changing the fuselage geometry and estimating drag using the procedure. The particular design alteration shown in Fig 28 increased fuselage volume while reducing zero-lift drag by 1½%. A combination of changes, such as straightening the

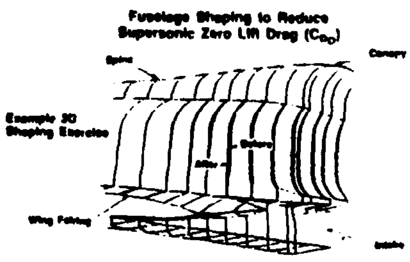

Fig 28 Full Shaping - Reduced C_{D0} by 8%
Exercise Increased Volume by 400 Litres

spine, waisting the fuselage sides, and increasing centre-fuselage volume, reduced zero lift drag by 5% and increased internal fuselage volume for fuel system etc by 400 litres.

Although largely superseded by recent developments in methods for solving the Euler equations, techniques such as GNFWD currently retain an important function in the design of supersonic combat-aircraft because they are

(a) economical in terms of computer time and

(b) simple to use and to understand.

4.2 Euler/panel program for wing/body configurations

While giving reasonable predictions for the flow over bodies, panel methods are not satisfactory for lifting surfaces, in general. Thus a hybrid procedure has been programmed by BAe (Warton) using an Euler code for the wing and a panel method for the body55. The method has been used to predict incremental drags and pitching moments (from surface pressure integrations) for a combat aircraft configuration due to wing camber and twist. Fig 29 shows that the procedure gives accurate predictions of the changes between two different wings over a relevant range of lift coefficients.

Trim drag is an important consideration in the design of combat aircraft for both subsonic and supersonic manoeuvres. Consequently a version of the hybrid method has been specifically developed at BAe to estimate the variation of zero-lift pitching moment with Mach number. This technique has been used in a design process to reduce the trim drag of a combat aircraft configuration, yielding a 6% reduction in lift-dependent drag at the critical subsonic and supersonic design points.

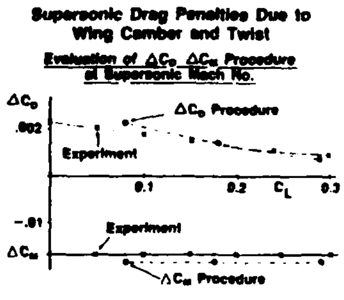

Fig 29 Increments Due to Wing Camber Changes on BAe Wind Tunnel Model

4.3 Euler methods for forebodies and pitot-intake cowls

The BAe Euler code for axisymmetric forebodies[26] has been used to calculate the variation of drag with Mach number at low supersonic speeds for the forebody of Fig 22 at zero incidence. Fig 22 shows that the method provides a reasonably faithful representation of the variation for Mach numbers between 1 and 1.2.

As noted in section 4, calculations have been made of cowl pressure drag by a version of the BAe Euler code26 for pitot cowls (Fig 24) at supersonic speeds. Fig 25 shows that predictions by this method are in good agreement with measurement.

4.4 Euler/Multiblock method

Although methods such as those described in section 4.1 and 4.2 have demonstrated their usefulness as engineering tools, increasing use will be made in the future of methods such as the ARA/BAe Euler/Multiblock code, as noted in section 3.5. The application of this method to wing/body configurations representative of supersonic combat aircraft is described and assessed in Ref 56. In this study, drag is determined by the 'local' method and thus needs to be regarded with caution because of the sensitivity of the method to discretisation errors. A study has been made of the effect on drag of grid structure and density but this was not conclusive56. Therefore the assessment of the method has been based mainly upon comparisons with measurements of wing pressure distributions and overall forces made on two half models. In order that the comparison is not affected by extraneous effects, such as these due to the interaction between the half body and the sidewall boundary layer, overall force measurements on the body alone are subtracted from those of the wing/body configuration at each angle of incidence and an analogous procedure is used in the calculation by the CFD method. Comparisons are shown in Fig 30 for M = 1.6 and for one of the wings studied, the calculated value of drag coefficient having been increased by 0.0054 to allow for skin friction (assumed to be unaffected by wing incidence, thickness and camber). The agreement between calculation and measurement is, on the whole, fair. Differences between prediction and measurement of lift at angles of incidence above about 6° can be explained by the effects of shock-induced separation not simulated in the calculation method. The obvious discrepancies between calculation and measurement of drag at low lift is believed to be due mainly to inaccurate predictions of suction near the leading-edge.

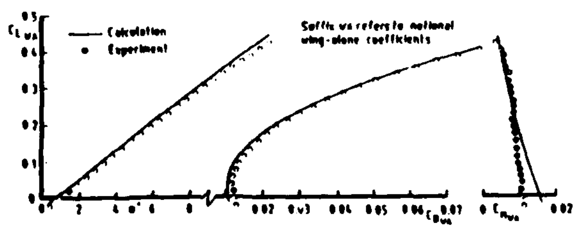

Fig 30 Overall lift, drag and pitching moment comparison between theory and experiment. M = 1.6, Wing A

4.5 Hall's multigrid method

Woodward[57] has used Hall's multigrid method[77] for solving the Euler equation, previously mentioned in section 3.1, to study the wave drag of aerofoils with rounded leading-edges at supersonic free stream speeds. This method is particularly suitable for studying flows of this kind since it has an unusually large number of grid points in the leading-edge region and is thus able to represent accurately the strong detached shock and the rapid spatial changes in the flow near the leading edge.

Fig 31 illustrates some of the results obtained by Woodward for wave drag by the 'local' method and shows the effect on the variation of wave drag with lift of changing nose radius. At zero lift an optimum nose radius of about 1½% chord is obtained but, as lift increases, the optimum value becomes smaller. This interesting result illustrates well the ability of CFD to provide relatively rapid assessments of drag differences due to changes in shape and the means of determining drag optima.

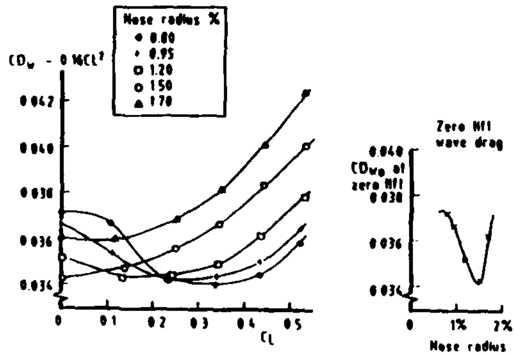

Fig 31 Calculated variation of wave drag with lift for varying nose - radius aerofoils. M = 1.1

5 CONCLUDING REMARKS

This paper has shown that, while the wholly theoretical prediction of aircraft drag is not yet possible, CFD methods exist in UK for drag prediction which are of considerable value to the aircraft designer in the following tasks:

- selection of the shape of aircraft components at the preliminary stages of the design;
- analysis of drag and diagnosis of sources of unwanted drag;
- 'extrapolation' of wind-tunnel drag data to 'full scale'.

Further refinements are needed to numerical methods for solving the Euler equation to reduce the sensitivity of drag predictions by these methods to grid density. Such developments would allow multiblock schemes to be exploited to calculate the drag of complex configurations, and, as such, would be a step in the direction away from the current dependence on wind-tunnel tests.

UK methods of solving the Reynolds-averaged, Navier-Stokes equation have yet to make a significant impact as techniques for drag prediction. Future developments in this area depend mainly on improvements being made to the turbulence models used, and the prospects of these being effected in the near term are uncertain. Thus viscous/inviscid inter-action techniques are expected to continue to feature prominently in UK drag prediction methods for some time to come.

REFERENCES

1 S. P. J. Butler. Technical evaluation report. AGARD-CP-124, Aerodynamic drag 1973.

2 F. R. Bailey, W. F. Ballhaus Jr. A large-scale computer facility for computational aerodynamics. IEEE Transactions on Nuclear Science Vol NS-32 No 1 February 1985.

3 N. J. Yu, H. C. Chen, S. S. Samant, P. E. Rubbert. Inviscid drag calculations for transonic flows. AIAA Paper 83-1928 (1983).

4 R. C. Lock. Prediction of the drag of wings at subsonic speeds by viscous/inviscid interaction techniques Paper 10 AGARD-R-723 1985.

5 C. M. Billing, A. J. Bocci. The MACHCONT method for calculating the wave drag of a 2D aerofoil. ARA Memorandum 272 (1986).

6 S. E. Allwright. Calculation of wave drag by analysis of 3D transonic flow field solutions. BAe unpublished Report.

7 C. C. L. Sells. Solution of the Euler equations for transonic flow past a lifting aerofoil. RAE Technical Report 80065 (1980).

8 P. R. Ashill, J. L. Fulker. Calculation of the viscous and vortex drag components of wing/body configurations. RAE Technical Report 87028 (1987).

9 R. C. Lock, B. R. Williams. Viscous/inviscid interactions in external aerodynamics. Prog Aerospace Sci Vol 24 pp 51-171. Pergamon Journals Ltd (1987).

10 B. R. Williams, The prediction of separated flow of using a viscous-inviscid interaction method. ICAS Paper 84-2.3.3 (1984).

11 J. E. Green, D. J. Weeks, J. W. F. Brooman. Prediction of turbulent boundary layers and wakes in compressible flow by a lag-entrainment method. ARC R&M 3791 (1977).

12 B. Thwaites. Approximate calculation of the laminar boundary layer. Aero, Qu., 1, 245 (1949).

13 P. R. Ashill, R. F. Wood, D. J. Weeks. An improved, semi-inverse version of the viscous Garabedian and Korn method VGK. RAE Technical Report 87002 (1987).

14 D. J. Butler, B. R. Williams. The development and application of a method for calculating the viscous flow about high-lift aerofoils. AGARD-CP-291. Paper No 25 (1980).

15 B. R. Williams, D. S. Woodward. Multiple Aerofoil Viscous Iterative System (MAVIS), the initial structure and possible extensions. RAE Technical Memorandum Aero 1632 (1975).

16 J. C. Newling. An improved two-dimensional multi-aerofoil program. HSA-MAE-R-FDM-0007 (1977).

17 H. P. A. H. Irwin. A calculation method for the two-dimensional turbulent flow over a slotted flap. ARC CP-1267 (1974).

18 A. G. T. Cross. BAe unpublished work.

19 D. A. King, B. R. Williams. Developments in computational methods for high-lift aerodynamics. Paper presented at Royal Aeronautical Society symposium 'High Lift Aerodynamics', Churchill College, Cambridge, 15-16 December 1986.

20 N. P. Weatherill, L. J. Johnston, A. J. Peace, J. A. Shaw. A method for the solution of the Reynolds-averaged Navier-Stokes equations on triangular grids. Paper presented at 7th GAMM Conference on Numerical Methods in Fluid Mechanics, Louvain-La-Neuve, Belgium September 9-11 1987.

21 M. R. Collyer, R. C. Lock. Prediction of viscous effects in steady transonic flow past an aerofoil. Aero, Qu., 30, 485 (1975).

22 A. F. Jones, M. C. P. Firmin. RAE unpublished Report.

23 P. R. Ashill, D. J. Weeks, J. L. Fulker. Wind Tunnel experiments on aerofoil models for the assessment of computational flow methods. To be presented at AGARD FDP Conference 'Validation of computational fluid dynamics' Lisbon May 1988.

24 P. R. Ashill. RAE unpublished work.

25 A. Jameson, W. Schmidt, E. Turkel. Numerical solutions of the Euler equations by finite volume methods using Runge-Kutta time stepping schemes. AIAA Paper 81-1259, 1981.

26 R. H. Doe, A. Pagano, T. W. Brown. The development of practical Euler methods for aerodynamics design. ICAS 86 5.5 (1986).

27 M. G. Hall. Cell vertex multigrid schemes for solution of the Euler equations. RAE Technical Memorandum Aero 2029 (1985).

28 L. J. Johnston. Some preliminary results from a prediction method for the viscous flow around aerofoil sections. ARA Memo 281 (1987).

29 A. Roberts, K. Rundle. Computation of incompressible flow about bodies and thick wings using the spline mode system. BAC (Weybridge) Report Aero MA19, 1972, ARC 33775.

30 A. Roberts, K. Rundle. The computation of first order compressible flow about wing/body combinations. BAC (Weybridge) Report Aero MA20, 1973.

31 D. Hunt. The panel method for subsonic aerodynamic flows. A survey of mathematical formulations and numerical models, and an outline of the new British Aerospace scheme. VKI LS 1978-4, Brussels, March 13-17, 1978.

32 J. A. H. Petrie. A surface source and vorticity panel method. Aero. Qu., 29 251 (1978).

33 A. G. T. Cross. Calculation of compressible three-dimensional turbulent boundary layers with particular reference to wings and bodies. British Aerospace (Brough) Report YAD 3379 (1979).

34 C. M. Albone, M. G. Hall, G. Joyce. Numerical solutions for transonic flows past wing-body combinations. RAE TM Aero 1645 (1975).

35 M. C. P. Firmin. Calculation of transonic flow over wing-body combinations with an allowance for viscous effects. AGARD-CP-291, Paper 8 (1981).

36 C. R. Forsey, M. P. Carr. The calculation of transonic flow over three-dimensional swept wings using the exact potential equation. DGLR Symposium on 'Transonic Configurations', DGLR Paper 78-064 (1978).

37 M. T. Arthur. A method for calculating subsonic and transonic flow over wings and wing-fuselage combinations with an allowance for viscous effects. AIAA-84-0428 (1984).

38 D. Isaacs. A two-dimensional panel method for calculating slender-body theory loading (or loading for minimum vortex drag) on a body of arbitrary cross section. RAE TR 81003 (1983).

39 P. R. Ashill, P. D. Smith. An integral method for calculating the effect on turbulent boundary-layer development of sweep and taper. The Aeronautical Journal pp 45-51, Feb (1985).

40 P. D. Smith. An integral prediction method for three-dimensional compressible turbulent boundary layers. ARC R&M 3738 (1972).

41 M. D. Hodges, P. R. Ashill, P. D. Cozens, R. C Lock. Application to a particular model of an approximate theory for determining the spanwise distribution of and total wave drag on a swept wing. UK MOD unpublished Report.

42 D. F. Myring. A theoretical study of body drag in subcritical axisymmetric flow. Aero. Qu., 27 (3) (1976).

43 T. J. Baker, P. A. Ogle. A computer program to compute transonic flow over an axisymmetric solid body. ARA Memo No 197 (1977).

44 P. D. Cozens. The wave drag coefficient of spherically blunted secant ogive fore-bodies of fineness ratio 1.0, 1.5 and 2.0 at zero incidence in transonic flow ESDU TDM 83017 (1983).

45 B. M. Patel. Calculation of wave drag of spherically blunted secant ogive forebodies at low supersonic speeds using Euler codes. UK MOD unpublished Report.

46 N. P. Weatherill, J. A. Shaw. The simulation of inviscid flow around military forebody geometries using the Euler equations. ARA Memo No 269 (1986).

47 A. J. Peace. Transonic flow calculations around isolated inlet configurations. The Aeronautical Journal pp 103-110 March 1986.

48 E. L. Goldsmith. Forces and pressure distributions at subsonic and supersonic speeds on circular section pitot intakes. ARA Memo in preparation.

49 J. Hodges. A method for calculating subsonic flows over axisymmetric afterbodies including viscous and jet effects. RAE TR 82097 (1982).

50 L. E. Putnam, J. Hodges. Assessment of NASA and RAE viscous-inviscid interaction methods for predicting transonic flow over nozzle afterbodies. AIAA-83-1789 (1983).

51 A. J. Peace. The calculation of axisymmetric afterbody flows with jet effects by a viscous/inviscid interaction method. ARA Report 67 (1986).

52 D. E. Reubush, J. F. Runckel. Effect of fineness ratio on boattail drag of circular-arc afterbodies having closure ratios of 0.5 with jet exhaust at Mach numbers up to 1.3. NASA TN D-7192 (1973).

53 N. P. Weatherill, J. A. Shaw, C. R. Forsey, K. E. Rose. A discussion on a mesh generation technique applicable to complex geometries. AGARD Symposium on Applications of computational fluid dynamics in aeronautics, Aix-en-Provence, France, April 1986.

54 N. P. Weatherill, C. R. Forsey. Grid generation and flow calculation for aircraft geometries. J Aircraft, Vol 22 No 10, Oct 1985.

55 W. R. Marchbank. The integration of computational fluid dynamics into the military aircraft design process. Paper 11 AGARD-CP-412 1986.

56 J. L. Fulker, P. R. Ashill. A theoretical and experimental evaluation of a numerical method for calculating supersonic flows over wing/body configuration. To be presented at AGARD FDP Conference 'Validation of computational fluid dynamics'.

57 P. S. Woodward. RAE unpublished work.

ACKNOWLEDGMENTS

The cooperation of all those who responded to requests for information is gratefully acknowledged as is the work by Mrs N E Rycroft and Mr G L Riddle in preparing the figures.

REPORT DOCUMENTATION PAGE

Overall security classification of this page

UNLIMITED

As far as possible this page should contain only unclassified information. If it is necessary to enter classified information, the box above must be marked to indicate the classification, e.g. Restricted, Confidential or Secret.

1. DRIC Reference (to be added by DRIC)	2. Originator's Reference	3. Agency Reference	4. Report Security Classification/Marking
	RAE Aero 2146	N/A	UNLIMITED

5. DRIC Code for Originator	6. Originator (Corporate Author) Name and Location
7672000H	Royal Aerospace Establishment, Bedford, Beds, UK
5a. Sponsoring Agency's Code	**6a. Sponsoring Agency (Contract Authority) Name and Location**
N/A	N/A

7. Title CFD methods for drag prediction and analysis currently in use in UK

7a. (For Translations) Title in Foreign Language

7b. (For Conference Papers) Title, Place and Date of Conference

8. Author 1. Surname, Initials	9a. Author 2	9b. Authors 3, 4	10. Date	Pages	Refs.
Ashill, P. R.			October 1988	21	57
11. Contract Number	**12. Period**	**13. Project**	**14. Other Reference Nos.**		

15. Distribution statement

(a) Controlled by –

(b) Special limitations (if any) –

If it is intended that a copy of this document shall be released overseas refer to RAE Leaflet No.3 to Supplement 6 of MOD Manual 4.

16. Descriptors (Keywords) (Descriptors marked * are selected from TEST)

Drag prediction.

17. Abstract

Computational methods developed in UK for the prediction of the drag of aircraft components at subsonic and supersonic speeds are critically reviewed. In many cases, the flow modelling is found to be lacking in certain respects. Despite this, however, the review suggests that these methods have a useful function both in the early stages of aircraft design, when they may be used to study differences in the drag of various shapes, and later in support of wind-tunnel tests as a diagnostic tool and also to 'extrapolate' the data to 'full scale'.